Patterns of Gene Expression During *Drosophila* Mesoderm Development

Eileen E. M. Furlong,[1] Erik C. Andersen,[1]* Brian Null,[1] Kevin P. White,[2]† Matthew P. Scott[1]‡

The transcription factor Twist initiates *Drosophila* mesoderm development, resulting in the formation of heart, somatic muscle, and other cell types. Using a *Drosophila* embryo sorter, we isolated enough homozygous *twist* mutant embryos to perform DNA microarray experiments. Transcription profiles of *twist* loss-of-function embryos, embryos with ubiquitous *twist* expression, and wild-type embryos were compared at different developmental stages. The results implicate hundreds of genes, many with vertebrate homologs, in stage-specific processes in mesoderm development. One such gene, *gleeful*, related to the vertebrate *Gli* genes, is essential for somatic muscle development and sufficient to cause neural cells to express a muscle marker.

Formation of muscles during embryonic development is a complex process that requires coordinate actions of many genes. Somatic, visceral, and heart muscle are all derived from mesoderm progenitor cells. The *Drosophila twist* gene (*1*), which encodes a bHLH transcription factor, is essential for multiple steps of mesoderm development: invagination of mesoderm precursors during gastrulation (*2*), segmentation (*3*), and specification of muscle types (*4*). The role of *twist* in mesoderm development has been conserved during evolution (*5*), perhaps because it controls conserved regulatory mesoderm genes. For example, *tinman* and *dMef2* are regulated by Twist in flies (*6*, *7*) (Fig. 1A) and are highly conserved in sequence and function in vertebrates (*8*–*10*).

In *Drosophila*, somatic muscle forms from progenitor cells that divide to become muscle founder cells (*11*). Founder cells acquire unique identities controlled by transcription factors including *Krüppel*, *S59*, *vestigial*, and *apterous*. Each of the 30 body wall muscles in an abdominal hemisegment is initiated by a single founder cell and has unique attachments and innervations (*12*). To further clarify mechanisms underlying founder cell specification, myoblast fusion, and muscle patterning, we have used *Drosophila* mutants together with microarrays of cDNA clones.

[1]Departments of Developmental Biology and Genetics, Howard Hughes Medical Institute, Beckman Center B300, [2]Department of Biochemistry, 279 Campus Drive, Stanford University School of Medicine, Stanford, CA 94305–5329, USA.

*Present address: Mail Stop 68-425 Department of Biology, Massachusetts Avenue, Cambridge, MA 02139, USA

†Present address: Department of Genetics, Sterling Hall of Medicine, 333 Cedar Street, Yale University School of Medicine, New Haven, CT 06520, USA.

‡To whom correspondence should be addressed. E-mail: scott@cmgm.stanford.edu

Transcription profile of twist *homozygous mutant embryos. twist* mutant embryos develop no mesoderm (*1*) [Web fig. 1 (*13*)]. We compared the population of mRNA species isolated from *twist* homozygous embryos with that of stage-matched wild-type embryos. *Drosophila* lethal mutations are maintained as heterozygotes, in trans to balancer chromosomes. A *twist* mutation was established in trans to a balancer chromosome carrying a transgene encoding green fluorescent protein (*GFP*) (*14*). Embryos were collected from wild-type and *twist/GFP*-balancer fly stocks at specific developmental stages. The *twist/GFP*-balancer collections contain a mixed population of embryos: one-quarter *twist* homozygotes lacking *GFP*, half heterozygotes with one copy of *GFP*, and one-quarter homozygous for the balancer chromosome with two copies of *GFP*. Homozygous *twist* mutant embryos were separated from their siblings using an embryo sorter (*15*) [Web fig. 2 (*13*)]. Putative homozygous *twist* embryos were assessed by immunostaining with an antibody to dMef2. More than 99% of the selected embryos had the *twist* phenotype.

Three different periods of mesoderm development were analyzed: stages 9-10, 11, and 11-12 [stages according to (*16*)]. During stage 9-10, the earliest time *GFP* is detectable in the balancer embryos (*14*), mesoderm cells migrate dorsally and become specified as somatic, visceral, cardiac, and fat body mesoderm. *twist* and its direct targets *tinman* and *dMef2* are expressed throughout stage 9-10 mesoderm. The middle period contained stage 11 embryos and is a transition between the first period (stage 9-10) and the third period (late stage 11-12). During late stage 11 and stage 12, myoblast fusion begins and *twist* expression remains prominent in only a subset of the somatic muscle cells.

For each developmental period, three independent embryo collections, embryo sortings, and microarray hybridizations were conducted. The microarrays used for the analysis contained over 8500 cDNAs corresponding to 5081 unique genes plus a variety of controls [see Web fig. 3 for array details (*13*)]. Each embryonic RNA sample was compared with a reference sample, which contains RNA made from all stages of the *Drosophila* life cycle and allows direct comparisons among all the experiments. Sample and array variability was determined by calculating correlation coefficients and standard deviations for each gene for all pair-wise combinations of repeated samples. The median correlation coefficient is 0.92, and median standard deviation divided by mean is 0.246 [see Web text for validation information (*13*)].

To determine how transcription was affected by the *twist* mutation, SAM (significance analysis of microarrays) analysis was used (*17*). Genes that are normally highly expressed in mesoderm should have lower transcript levels in *twist* homozygotes. Genes in other tissues whose expression depends on signals from the mesoderm might also have reduced expression. Transcripts of 130 genes, the "Twist-low" group, were significantly lower in *twist* mutants than in wild type (Fig. 2A). Conversely, cells that would have formed mesoderm may take on other fates in the absence of *twist*, such as neuroectoderm; therefore, many transcript levels could increase in *twist* mutants. Genes whose transcription is repressed by signals from the mesoderm would also be enriched in *twist* mutants. One hundred fifty genes, called the "Twist-high" group, have increased levels of RNA in *twist* mutant embryos (Fig. 2A).

In total, 280 of ~5000 genes had significant changes in transcript levels, with 10 false positives (*17*) [see Web text for validation information (*13*)]. The genes on the array include 15 previously characterized mesoderm-specific genes, all of which were significantly reduced in *twist* mutant embryos (Fig. 3A). The arrays also contain genes known to be transcribed in both mesoderm and other cell types. Significant changes in expression were detected for many of these genes (Fig. 3B).

The 130 Twist-low genes were divided into three groups (A, B, and C) with similar trends of expression by a self-organizing map (SOM) clustering program (Fig. 1B) (*18*). The 24 group A genes, which included *tinman*, *dMef2*, and *bagpipe*, had reduced transcript levels in *twist* mutants at all developmental stages assayed. Most of the Twist-low genes fall into the B and C groups. The 62 group B "early genes" encode transcripts with reduced levels of expression in *twist* mutants only during stages 9-10, not later. One member of group B, *stumps* (*dof/hbr*) is

essential for mesoderm cell migration. *stumps* RNA is abundant in the mesoderm at stages 9-10 and is strongly reduced by stage 11 (Fig. 1B) (*19*). At stage 11, *stumps* RNA accumulates in trachea, which are largely unaffected in *twist* mutants.

The 44 group C genes have reduced transcript levels in *twist* mutant embryos only during late stage 11 and stage 12. These "late genes" include *blown fuse*, a gene essential for myoblast fusion (*20*); *delilah*, a gene required for somatic muscle attachment (*21*); and genes such as *kettin*, which is required to form contractile muscle (*22*). Given the predominantly early expression of *twist*, the early genes in groups A and B are the best candidates for direct transcription targets of Twist, though some indirectly activated genes may be present within these groups. Group C late genes are likely to be regulated by products of genes that are activated by Twist.

In situ hybridizations were done using a previously uncharacterized representative of each Twist-low group (Fig. 1C). In each case, the hybridization pattern was consistent with the predicted time of transcription. A group A gene, CG15015 (GH16741), is transcribed in somatic muscle throughout stages 9-12. A group B gene, CG12177 (GH22706), is transcribed during early mesoderm development, but not later. CG14848 (GH21860), a group C gene, is expressed in the stomodeum but not the mesoderm during stages 9-10. Its mesoderm expression initiates during stage 11, the latest period of the *twist* experiment. Thus, combining loss-of-function mutant embryo analysis with staged embryo collections provides gene expression information for both tissue specificity and temporal expression.

A complementary test: The transcription profile with twist overexpression. The misexpression of *twist* in the ectoderm is sufficient to convert both neuronal and epidermal tissues to a myogenic cell fate (*4*). RNA from embryos with ubiquitous *twist* expression was used to evaluate the ability of Twist to initiate mesoderm-like gene expression in cells that would normally form other tissue types. Genes whose transcript levels decrease in *twist* loss-of-function embryos and increase when *twist* is ubiquitous are excellent candidates for regulators of mesoderm development or differentiation.

To ectopically express *twist*, a dominant gain-of-function mutation of the maternal gene *Toll* (*Toll*^{10B}) was used (*23*). Activated Toll induces the expression of *twist* and *snail* in early embryos and of immune response genes in older embryos (Fig. 1A) (*24*, *25*). Thus, the effects of *Toll*^{10B} on gene expression reflect the activities of Twist as well as Snail and Dorsal, or their combined actions. *Toll*^{10B} embryos are essentially bags of mesoderm; epidermal structures are absent or greatly reduced (*23*), and they have been used successfully in subtractive hybridization screens to identify mesoderm genes (*26*). We compared the gene transcription profile of *Toll*^{10B} embryos with that of wild-type embryos during four periods of development, using the reference sample to normalize experiments. The earliest period, stage 5, is when *twist* is initially expressed in presumptive mesoderm. The other three periods analyzed were those used in the *twist* mutant analysis: stages 9-10, 11, and 11-12.

In *Toll*^{10B} embryos, 447 genes had significant changes in RNA levels compared with stage-matched wild-type embryos (Fig. 2A), 16 of which are predicted to be false positives (*17*) [see Web text for validation information (*13*)]. Transcripts from 166 genes were reduced in *Toll*^{10B} embryos compared with wild type. These genes may be involved in neuroectoderm events that are blocked when cells are turned into mesoderm (Fig. 2, clusters B and C). Transcripts of 281 "Toll-high" genes were increased in *Toll*^{10B} embryos. Of the 21 previously characterized mesoderm-specific genes on the arrays, 18 have significantly increased transcript levels in *Toll*^{10B} embryos (Fig. 3A). The remainder may require activators other than *Toll*, such as signals from the severely altered ectoderm.

Mesoderm and non-mesoderm gene classes. Genes with altered transcription in *twist* and *Toll*^{10B} mutants were analyzed with a hierarchical clustering program (*27*) to identify similar transcription profiles. The genes were divided into putative "mesoderm" and "non-mesoderm" groups (Fig. 2A). Non-mesoderm genes were defined as having increased transcript levels in mesoderm-deficient (*twist*) embryos and/or decreased expression in mesoderm-enriched (*Toll*^{10B}) embryos (Fig. 2, B and C). Mesoderm genes were defined as having decreased transcript levels in *twist* mutants and/or increased transcripts in *Toll*^{10B} mutants (Fig. 2, D through F). The mesoderm genes group will also contain genes expressed in other tissues in a mesoderm-dependent manner.

Non-mesoderm genes in clusters B and C are repressed in *Toll*^{10B} mutants. Cluster B (Fig. 2B) genes have increased RNA levels in *twist* mutant embryos, whereas cluster C (Fig. 2C) genes do not change significantly. The overexpression of *twist* in the presumptive ectoderm in *Toll*^{10B} embryos results in a conversion of ectodermal cell fate into mesoderm. *snail* and *dorsal* are ectopically expressed in *Toll*^{10B} embryos (Fig. 1A) and transcriptionally repress the expression of neuroectoderm and ectoderm genes (*28*, *29*). The conversion of ectoderm to mesoderm due to *twist* misexpression, and the ability of

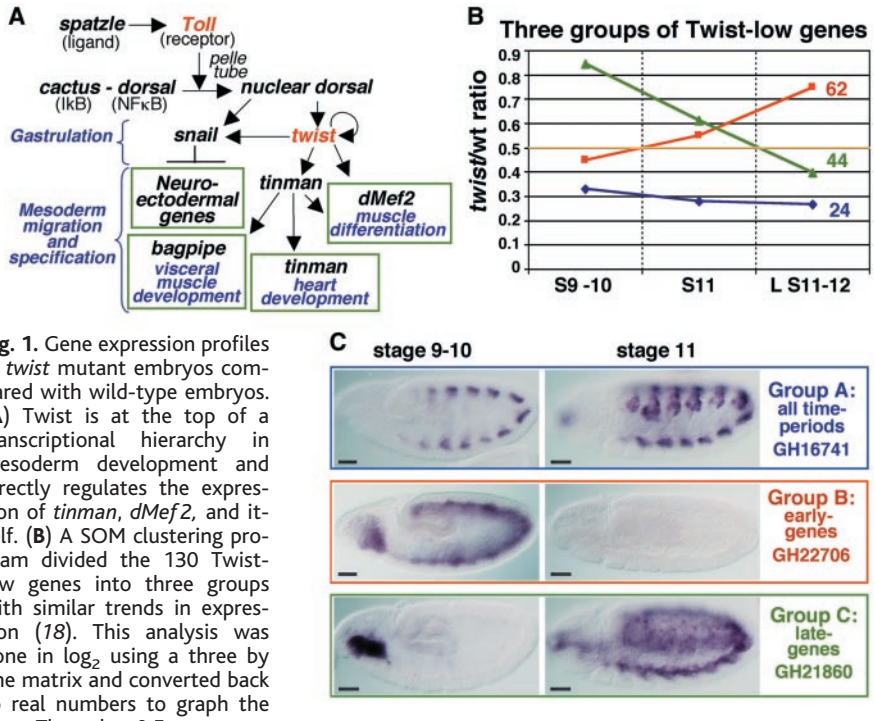

Fig. 1. Gene expression profiles in *twist* mutant embryos compared with wild-type embryos. (**A**) Twist is at the top of a transcriptional hierarchy in mesoderm development and directly regulates the expression of *tinman*, *dMef2*, and itself. (**B**) A SOM clustering program divided the 130 Twist-low genes into three groups with similar trends in expression (*18*). This analysis was done in $\log_2$ using a three by one matrix and converted back to real numbers to graph the data. The value 0.5 represents a twofold reduction in *twist* embryos compared with wild type. Increasing the complexity of the SOM matrix subdivides these subgroups further (e.g., three by two matrix), but the general trends remain the same. Graph lines represent average transcription changes for all genes within that group. Blue diamond, group A; red square, group B; green triangle, group C. S9-10, stage 9-10; S11, stage 11; L S11-12, late stage 11 to 12. Web table 1 (*13*) shows the genes within groups A through C. (**C**) In situ hybridization with one unknown gene from each group in (B). Scale bars in each panel of (C) are 39 μm.

Snail and Dorsal to repress ectoderm genes, suggests that the B and C clusters should contain primarily neuroectodermal genes. Indeed, the non-mesoderm genes include 31 previously characterized neuroectodermal genes. One previously unknown cluster B gene that encodes a putative cell adhesion protein is transcribed in the ventral nerve cord (Fig. 2B). Another previously unknown gene within cluster C is transcribed within the developing brain (Fig. 2C).

The Twist-low and Toll-high genes have in common 51 genes (Fig. 2A) that are highly likely to be involved mesoderm development. For example, transcription of the genes in cluster D (Fig. 2D) is reduced in *twist* mutants and increased in *Toll*^{10B} mutants during most or all time periods.

A complete overlap between Twist-low and Toll-high gene sets is not expected for three reasons, as follows: (i) Development of dorsal mesoderm, and of muscle founder cells marked by *apterous* and *connectin*, requires the Decapentaplegic (a transforming growth factor-β–class signal) (*30, 31*) and perhaps others. Changed characteristics of cells that form ectoderm in *Toll*^{10B} embryos

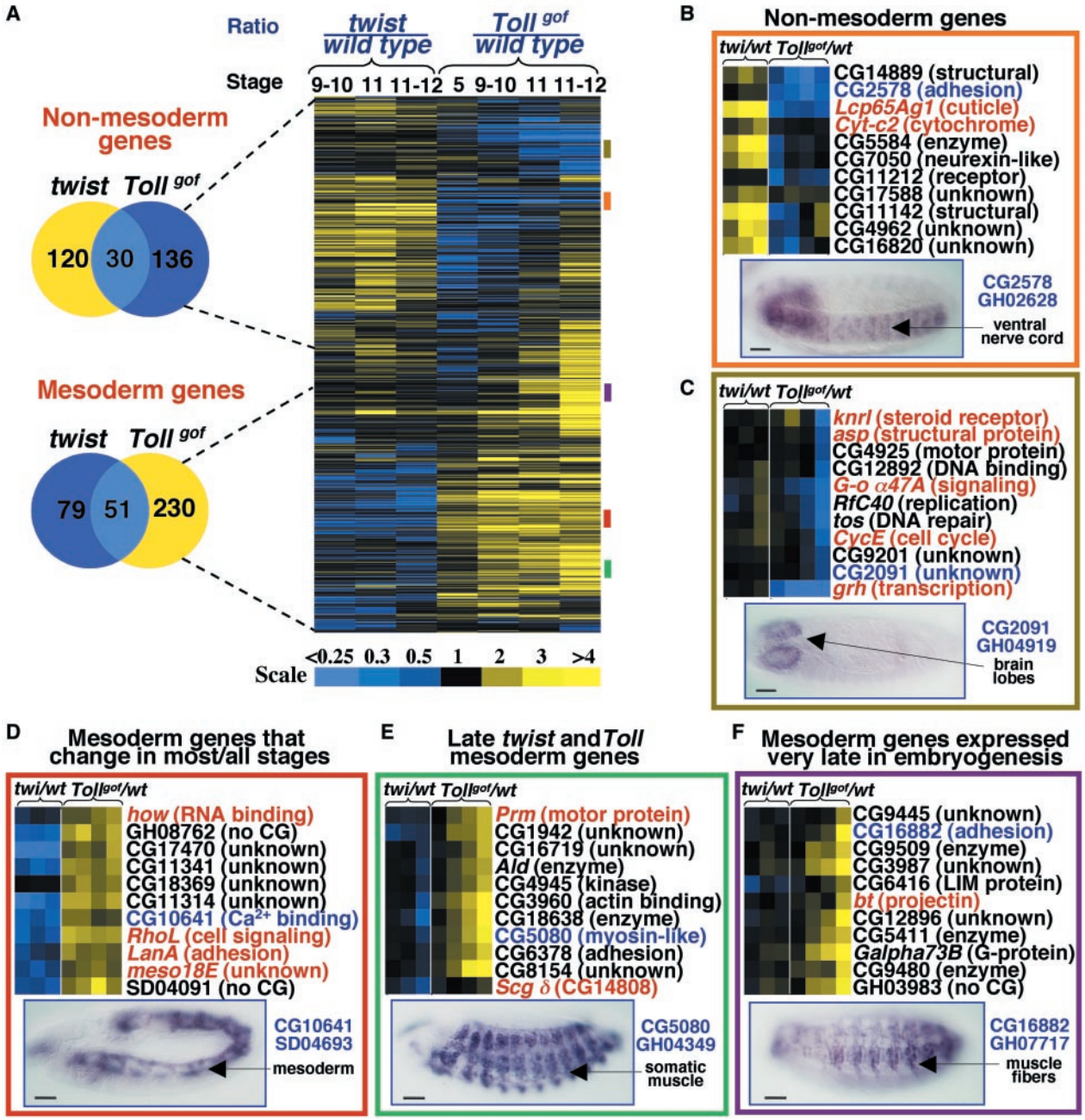

Fig. 2. A comparison of gene expression profiles of mesoderm-deficient (*twist* mutant) and mesoderm-enriched (*Toll*^{10B} mutant) embryos. (**A**) Compared with wild type, 643 genes had significantly changed transcription in *twist* and *Toll* mutant embryos. Ratios of mutant/wild type were arranged with a hierarchical clustering program, and the results are shown in Web fig. 3 (*13, 27*). The Venn diagram shows the overlap between the *twist* and *Toll* experiments. The example clusters [(B) through (F)] are indicated by the colored bars in (A) and colored box around the corresponding cluster in (B) through (F). A white line in the diagram between the *twist* and *Toll* experiments marks the transition in the clusters between the two genotypes. Examples of non-mesoderm gene clusters are shown in (**B** and **C**). Three representative clusters for mesoderm genes are shown in (**D** through **F**). Red typeface indicates either genes known to be transcribed in the nervous system and/or ectoderm [(B) and (C)] or known mesoderm genes [(D) through (F)]. One unknown gene (blue typeface) from each cluster was selected for in situ hybridization. Scale bars in (B) through (F) are 39 μm.

interferes with these signaling events. We observe a significant reduction in *dpp* RNA levels in *Toll*^{10B} embryos (Web Fig. 3). (ii) During midgut development, endoderm cells migrate along the mesoderm. Midgut endoderm development is affected in *twist* mutants (*32*). Some Twist-low genes with unchanged expression in *Toll*^{10B} embryos are transcribed in the midgut (not shown). (iii) Ectopic Twist inhibits visceral mesoderm and heart development and promotes excess somatic muscle development (*4*). *Toll*^{10B} embryos produce high levels of Twist throughout the embryo, so genes that have reduced RNA levels in both *twist* and *Toll*^{10B} mutant embryos are likely to be visceral muscle and heart genes. Indeed, *bagpipe* and *connectin*, genes expressed in visceral mesoderm, are among the 79 Twist-low genes not induced by ectopic Twist (Fig. 3A).

Of the 281 Toll-high genes, 230 were unaffected in *twist* mutants. Some of the 230 are normally expressed late in embryogenesis in wild-type embryos but are expressed prematurely in *Toll*^{10B} embryos due to ectopic Twist. These include *Myo61F*, *MSP-300*, and *Paramyosin*, genes normally active in terminally differentiated muscle (stage 16) (Fig. 2F and Fig. 3A). Ectopic Snail and Dorsal in *Toll*^{10B} embryos may activate genes that are unaffected in *twist* mutants. Snail can repress neuroectodermal genes and may also activate mesoderm genes (*26*). Dorsal activates immune response genes later in development (*25*). *relish*, *drosomycin*, and *metchnikowin* genes—all immune response genes—have higher transcript levels in *Toll*^{10B} embryos.

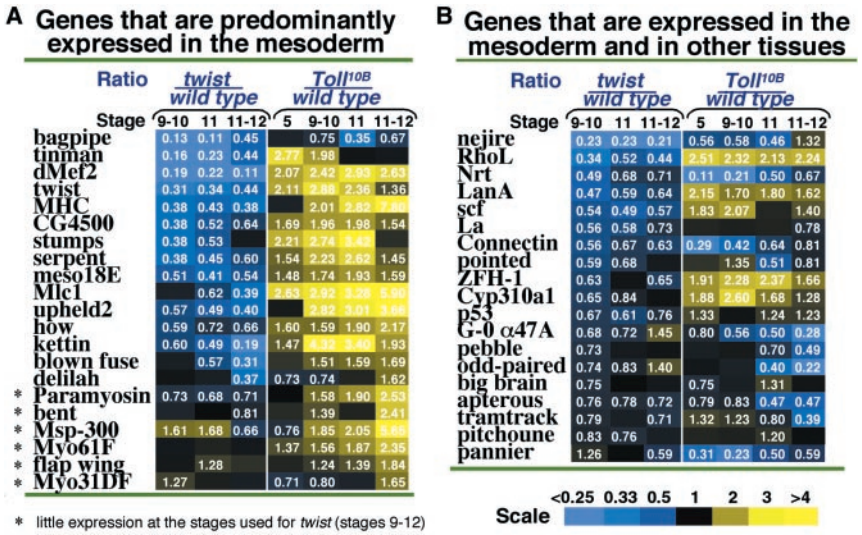

Fig. 3. (**A**) Changes in gene expression in *twist* and *Toll*^{10B} embryos compared with wild type for all known mesoderm-specific and muscle genes on the array. *stumps* was placed in this group because it is primarily expressed in the mesoderm during these stages. (**B**) Gene expression data for genes both in the mesoderm and other tissues.

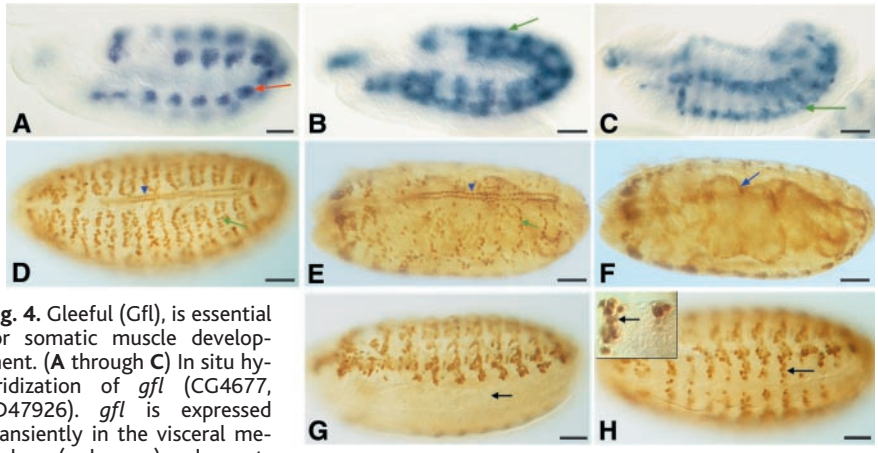

Fig. 4. Gleeful (Gfl), is essential for somatic muscle development. (**A** through **C**) In situ hybridization of *gfl* (CG4677, LD47926). *gfl* is expressed transiently in the visceral mesoderm (red arrow) and somatic mesoderm (green arrows) from stages 10-13. (**D**) Embryos injected with a control double-stranded RNA and immunostained with α-dMef2 antibody. (**E**) Embryos injected with double-stranded RNA for *gfl* (from LD47926 cDNA) and immunostained with α-dMef2. There is a severe loss of somatic muscle cells [green arrows in (D) and (E)]. (**F**) Same embryo shown in (E) focusing on visceral mesoderm (blue arrow). The heart [arrowheads in (D) and (E)] and visceral mesoderm appear normal. (**G**) Ventral view of a wild-type stage 16 embryo stained with α-dMef2. (**H**) Embryo containing *UAS-gfl* and *en*-GAL4 stained with α-dMef2. Ectopic expression of *gfl* induces dMef2 expression in the ventral nerve cord (black arrow). dMef2-expressing cells are embedded within the ventral nerve cord [inset in (H), 63× magnification]. Scale bars in (A) through (H)are 39 μm.

Data from loss- and gain-of-function experiments, combined with careful staging, yield a useful picture of genes that are likely to be required for mesoderm specification and muscle differentiation. Of 360 identified mesoderm genes, 273 have not been the focus of developmental studies. The predicted proteins encode transcription factors, signal transduction molecules, kinases, and pioneer proteins. The stage at which each gene is active is one criterion for assigning possible functions. Another key criterion will be finding a mutant phenotype. As a pilot, we have taken this additional step for the gene CG4677 (LD47926). Changes in CG4677 transcript levels were also observed in a *Toll*^{10B} subtractive hybridization screen (*26*).

gleeful*, a gene required for somatic muscle development.* CG4677 is transcribed in the visceral mesoderm at stages 10-13 and the somatic mesoderm during stages 11-13 (Fig. 4, A through C). This gene encodes a C_2H_2 zinc finger transcription factor with high sequence similarity to vertebrate Gli proteins, so we have named the gene *gleeful* (*gfl*). Mammalian Gli proteins act downstream of Hedgehog signaling proteins to control target gene transcription (*33*).

The role of *gfl* in mesoderm development was assessed by disrupting its function using RNA interference (*34*). Injection of a double-stranded RNA (dsRNA) control sequence had no effect on mesoderm development (Fig. 4D). In contrast, *gfl* dsRNA injection caused severe loss and disorganization of somatic muscle cells (Fig. 4E), whereas heart and visceral muscle were unaffected (Fig. 4, E and F). A similar phenotype was seen in *Df(3R)hh* homozygous embryos (not shown), the deficiency removes *gfl* but not the nearby *hedgehog* gene

To determine whether *gfl* can induce muscle cell development, a *UAS-gfl* transgenic fly strain was generated. Ectopic expression of *gfl* using an *en*-GAL4 driver results in lethality and induction of ectopic dMEF2 expression in the ventral nerve cord (Fig. 4H). Remarkably, Gfl is sufficient to induce expression of a muscle gene in neuronal cells. Previous studies have shown an essential role for Sonic hedgehog signaling in the formation of slow muscle in avian and zebrafish embryos (*35*, *36*). *gfl* may be performing a similar role in *Drosophila* somatic muscle development.

This study has combined mutant embryo

analyses with DNA microarrays to identify genes that are downstream of *twist* in mesoderm development. These efforts should be helpful in gaining a comprehensive view of cell fate determination, organogenesis, cell proliferation, and pattern formation in the mesoderm.

References and Notes

1. B. Thisse, M. el Messal, F. Perrin-Schmitt, *Nucleic Acids Res.* **15**, 3439 (1987).
2. M. Leptin, B. Grunewald, *Development* **110**, 73 (1990).
3. O. M. Borkowski, N. H. Brown, M. Bate, *Development* **121**, 4183 (1995).
4. M. K. Baylies, M. Bate, *Science* **272**, 1481 (1996).
5. J. Spring *et al.*, *Dev. Biol.* **228**, 363 (2000).
6. M. V. Taylor, K. E. Beatty, H. K. Hunter, M. K. Baylies, *Mech. Dev.* **50**, 29 (1995).
7. Z. Yin, X. L. Xu, M. Frasch, *Development* **124**, 4971 (1997).
8. N. D. Hopwood, A. Pluck, J. B. Gurdon, *Cell* **59**, 893 (1989).
9. C. Wolf *et al.*, *Dev. Biol.* **143**, 363 (1991).
10. S. M. Wang *et al.*, *Gene* **187**, 83 (1997).
11. M. V. Taylor, *Curr. Biol.* **10**, R646 (2000).
12. M. Bate, Ed., in *The Development of* Drosophila melanogaster (Cold Spring Harbor Laboratory Press, Plainview, NY, 1993), vol. II, pp. 1013–1090.
13. Web figures 1 through 3, Web table 1, and supplemental text are available at *Science* Online at www.sciencemag.org/cgi/content/full/1062660/DC1.
14. D. Casso, F. Ramirez-Weber, T. B. Kornberg, *Mech. Dev.* **91**, 451 (2000).
15. E. E. Furlong, D. Profitt, M. P. Scott, *Nature Biotechnol.* **19**, 153 (2001).
16. J. A. Campos-Ortega, V. Hartenstein, *The Embryonic Development of* Drosophila melanogaster (Springer-Verlag, Germany, 1997), pp. 9–84.
17. V. G. Tusher, R. Tibshirani, G. Chu, *Proc. Natl. Acad. Sci. U.S.A.* **98**, 5116 (2001).
18. P. Tamayo *et al.*, *Proc. Natl. Acad. Sci. U.S.A.* **96**, 2907 (1999).
19. S. Vincent, R. Wilson, C. Coelho, M. Affolter, M. Leptin, *Mol. Cell* **2**, 515 (1998).
20. S. K. Doberstein, R. D. Fetter, A. Y. Mehta, C. S. Goodman, *J. Cell. Biol.* **136**, 1249 (1997).
21. P. Armand, A. C. Knapp, A. J. Hirsch, E. F. Wieschaus, M. D. Cole, *Mol. Cell. Biol.* **14**, 4145 (1994).
22. A. Lakey *et al.*, *EMBO J.* **12**, 2863 (1993).
23. D. S. Schneider, K. L. Hudson, T. Y. Lin, K. V. Anderson, *Genes Dev.* **5**, 797 (1991).
24. M. P. Belvin, K. V. Anderson, *Annu. Rev. Cell. Dev. Biol.* **12**, 393 (1996).
25. I. Gross, P. Georgel, C. Kappler, J. M. Reichhart, J. A. Hoffmann, *Nucleic Acids Res.* **24**, 1238 (1996).
26. J. Casal, M. Leptin, *Proc. Natl. Acad. Sci. U.S.A.* **93**, 10327 (1996).
27. M. B. Eisen, P. T. Spellman, P. O. Brown, D. Botstein, *Proc. Natl. Acad. Sci. U.S.A.* **95**, 14863 (1998).
28. M. Leptin, *Genes Dev.* **5**, 1568 (1991).
29. M. Levine, *Cell* **52**, 785 (1988).
30. M. Frasch, *Nature* **374**, 464 (1995).
31. K. Staehling-Hampton, F. M. Hoffman, M. K. Baylies, E. Rushton, M. Bate, *Nature* **372**, 783 (1994).
32. R. Reuter, B. Grunewald, M. Leptin, *Development* **119**, 1135 (1993).
33. P. T. Chuang, T. B. Kornberg, *Curr. Opin. Genet. Dev.* **10**, 515 (2000).
34. J. R. Kennerdell, R. W. Carthew, *Cell* **95**, 1017 (1998).
35. G. M. Cann, J. W. Lee, F. E. Stockdale, *Anat. Embryol.* **200**, 239 (1999).
36. K. E. Lewis, *et al.*, *Dev. Biol.* **216**, 469 (1999).

37. We thank E. Johnson, M. Arbeitman, B. Baker, M. Siegal, R. Tibshirani, and V. Goss Tusher for statistical advice; B. Baker, F. Imam, and G. Zimmermann for careful manuscript reading; and M. Arbeitman, F. Imam, and E. Johnson for collaborating to prepare the arrays and reference sample. Support for E.F. by European Molecular Biology Organization and Stanford Berry Fellowships, B.N. by NSF, and K.W. by Helen Hay Whitney fellowships. The research was supported by NIH grant K22 HG00045-02 (K.W.) and HHMI and Defense Advanced Research Projects Agency grant MDA-972-00-1-0032 (M.S.).

18 May 2001; accepted 23 July 2001
Published online 2 August 2001;
10.1126/science.1062660
Include this information when citing this paper.

REPORTS

Origin of the Hard X-ray Emission from the Galactic Plane

Ken Ebisawa,[1]* Yoshitomo Maeda,[2,3] Hidehiro Kaneda,[3] Shigeo Yamauchi[4]

The Galactic plane is a strong emitter of hard x-rays (2 to 10 kiloelectron volts), and the emission forms a narrow continuous ridge. The currently known hard x-ray sources are far too few to explain the ridge x-ray emission, and the fundamental question of whether the ridge emission is ultimately resolved into numerous dimmer discrete sources or truly diffuse emission has not yet been settled. In order to obtain a decisive answer, using the Chandra X-ray Observatory, we carried out the deepest hard x-ray survey of a Galactic plane region that is devoid of known x-ray point sources. We detected at least 36 new hard x-ray point sources in addition to strong diffuse emission within a 17′ by 17′ field of view. The surface density of the point sources is comparable to that at high Galactic latitudes after the effects of Galactic absorption are considered. Therefore, most of these point sources are probably extragalactic, presumably active galaxies seen through the Galactic disk. The Galactic ridge hard x-ray emission is diffuse, which indicates omnipresence within the Galactic plane of a hot plasma, the energy density of which is more than one order of magnitude higher than any other substance in the interstellar space.

The Galactic ridge x-ray emission exhibits emission lines from highly ionized heavy elements such as Si, S, and Fe; hence, it may be considered to originate from optically thin hot plasmas with a temperature of several keV (*1*). If the plasma distribution is diffuse in the Galactic disk, the plasma temperature is higher than that which can be bound by Galactic gravity (*2*), and its energy density, ~ 10 eV/cm^3, is one or two orders of magnitude higher than those of other constituents in the interstellar space, such as cosmic rays, Galactic magnetic fields, and ordinary interstellar medium (*1, 3*). Another hypothesis is that the Galactic ridge x-ray emission is a superposition of numerous point sources (*4–7*). However, no class of x-ray objects is known with such a high plasma temperature and a large number density to satisfy the uniform surface brightness of the ridge emission (*3, 8*).

To resolve the origin of the Galactic ridge x-ray emission, we observed a "blank" region of the Galactic plane, $(l,b) \approx (+28°.45, -0°.2)$, where the Advanced Satellite for Cosmology and Astrophysics (ASCA) could not find any point sources (*3, 9*) brighter than $\sim 2 \times 10^{-13}$ erg s^{-1} cm^{-2} (2 to 10 keV). We used the Advanced CCD Imaging Spectrometer Imaging (ACIS-I) array on board the Chandra X-ray Observatory, with unprecedented sensitivity and imaging quality (Fig. 1). The observation was carried out on 25 and 26 February 2000, for a total exposure time of 90 ks. The pointing position was chosen because the direction is tangential to the Scutum arm where the ridge x-ray emission is strong.

We were interested in hard x-ray emission, so we searched in the 3- to 8-keV band to minimize the effects of Galactic absorption at lower energies and the intrinsic non–x-ray background in the higher energy band. The "wavdetect" source finding program in the Chandra data analysis package detected 53, 36, and 29 sources in the 17′ by 17′ ACIS-I field with 3σ, 4σ, and 4.5σ significance, respectively. For each of these sources, we determined the energy flux in the 2- to 10-keV band by fitting the energy spectrum after accounting for the position-dependent detector responses. The 3σ, 4σ, and 4.5σ thresholds roughly correspond to energy fluxes of $\sim 3 \times 10^{-15}$, $\sim 4 \times 10^{-15}$, and $\sim 5 \times 10^{-15}$ ergs s^{-1} cm^{-2} in the 2- to 10-keV band,